

Influence of relative humidity and physical load during storage on dustiness of inorganic nanomaterials: implications for testing and risk assessment

Marcus Levin · Elena Rojas · Esa Vanhala · Minnamari Vippola · Biase Liguori · Kirsten I. Kling · Ismo K. Koponen · Kristian Mølhave · Timo Tuomi · Danijela Gregurec · Sergio Moya · Keld A. Jensen

Received: 30 September 2014 / Accepted: 3 August 2015 / Published online: 13 August 2015
© Springer Science+Business Media Dordrecht 2015

Abstract Dustiness testing using a down-scaled EN15051 rotating drum was used to investigate the effects of storage conditions such as relative humidity and physical loading on the dustiness of five inorganic metal oxide nanostructured powder materials. The tests consisted of measurements of gravimetric respirable dustiness index and particle size distributions. Water uptake of the powders during 7 days of incubation was investigated as an explanatory factor of the changes. Consequences of these varying storage conditions in exposure modelling were tested using the control banding and risk management tool NanoSafer. Drastic material-specific effects on powder respirable dustiness index were observed with the change in TiO₂ from 30 % RH (639 mg/kg) to 50 %

RH (1.5 mg/kg). All five tested materials indicate a decreasing dustiness index with relative humidity increasing from 30 to 70 % RH. Test of powder water uptake showed an apparent link with the decreasing dustiness index. Effects of powder compaction appeared more material specific with both increasing and decreasing dustiness indices observed as an effect of compaction. Tests of control banding exposure models using the measured dustiness indices in three different exposure scenarios showed that in two of the tested materials, one 20 % change in RH changed the exposure banding from the lowest level to the highest. The study shows the importance of powder storage conditions prior to tests for classification of material dustiness indices. It also highlights the importance of correct storage information and relative humidity and expansion of the dustiness test conditions specifically, when using dustiness indices as a primary parameter for source strength in exposure assessment.

Electronic supplementary material The online version of this article (doi:10.1007/s11051-015-3139-6) contains supplementary material, which is available to authorized users.

M. Levin (✉) · K. Mølhave
Department of Micro and Nanotechnology, Technical University of Denmark, 2800 Kongens Lyngby, Denmark
e-mail: mle@nrcwe.dk

M. Levin · B. Liguori · K. I. Kling · I. K. Koponen · K. A. Jensen
National Research Centre for the Working Environment, Lersø Parkallé 105, 2100 Copenhagen, Denmark

E. Rojas · D. Gregurec · S. Moya
CIC biomaGUNE, Paseo Miramón 182 C,
20009 San Sebastián, Gipuzkoa, Spain

E. Vanhala · M. Vippola · T. Tuomi
Finnish Institute of Occupational Health, Topeliuksenkatu 41 A, 00250 Helsinki, Finland

M. Vippola
Department of Materials Science, Tampere University of Technology, Korkeakoulunkatu 6, 33720 Tampere, Finland

B. Liguori
Department of Environmental Engineering, Technical University of Denmark, 2800 Kongens Lyngby, Denmark

Keywords Dustiness · Rotating drum · Exposure assessment · Powder storage · Occupational health · Nanotechnology

Introduction

Handling of powders in workplaces is known to be associated with risk of dust release and may result in important occupational exposure levels (Brouwer 2010; Kuhlbusch et al. 2011). The production stage and powder handling is also the activity that causes the highest risk of occupational exposure to manufactured nanomaterials (Borm et al. 2006; Hämeri et al. 2009). To enable precautionary exposure management, different test methods have been established, which allows relative ranking of powders regarding their propensity to release dust; i.e. dustiness (Hamelmann and Schmidt 2005). Some dustiness test methods are fully standardized, such as the rotating drum and the continuous drop methods that were established in EN15051 (BS EN:15051 2006; Liden 2006). Currently new methods are underway under the CEN-NEN Mandate M437 to establish nano-specific dustiness test methods and measurement protocols, also considering the two test methods in EN15051 (Witschger et al. 2014).

To enable comparability in ranking, the standard dustiness methods are carefully harmonized regarding the mechanical design of the test systems, sampling design, as well as the conditions and measurement metrics to be used for quantification. In EN15051, the storage and experimental test conditions are set to room temperature and a relative humidity of 50 ± 10 %. However, workplace conditions are usually not controlled that well and in fact powder storage and handling is likely to take place under conditions relative far from the ideal testing conditions. Moreover, powders may be stored in different ways such as in small packs, drums, bags on palettes, big bags and silos, where the packed material may have been closed under vacuum or not. Consequently, powders may also be stored at great ranges in % RH and at high pressure gradients from top to bottom in a stack or silo. It is currently unclear how extensive such differences in humidity and storage pressure may affect different powders regarding their dustiness levels and dust characteristics.

Due to the general low number of workplace exposure measurement data, reliable early phase risk

assessment becomes more and more important (Aitken et al. 2011). Therefore, a better understanding of the uncertainties and recommendations for improvements of critical tests and input parameters needs to be identified as soon as possible to ensure that the precautionary approaches are still reliable and can consider worst case scenarios. Some REACH tools and new control banding-like tools are currently available for such conservative evaluations of which several use dustiness data as an indicator for the potential exposure or source strength (Liguori et al. Submitted; Brouwer 2012).

A previous study (Jensen et al. 2009) showed different effects on dustiness levels after 5 min of uniaxial low-pressure compaction (3.54 ± 0.14 kg/cm²) on a loose bentonite and granulated organoclay. The dustiness of the granulated organoclay increased after the uniaxial pressure load, whereas it was reduced in the case of the loose bentonite powders. Granulation is usually applied to improve the appearance, flow, mixing properties, of the powders as well as to decrease powder dustiness (Freitag and Kleinebudde 2003; Tardos 2005; Nishii and Horio 2007). It can be inferred that brief compaction of the bentonite in the study by Jensen et al. (2009) underwent some type of granulation, whereas the granulated organoclay was de-agglomerated resulting in reduced and increased dustiness, respectively.

Differences in the relative humidity (% RH) during powder storage may also change the characteristics of the emitted dust (Jensen et al. 2009). Intergranular fusion (caking) due to grain-particle-boundary dissolution–precipitation processes in partially water-soluble powder materials may occur in sufficiently humid air and durations of storage (Szepvolgyi et al. 2001; Gbureck et al. 2005; Brockel et al. 2006). Such processes may initially result in agglomerates of softly bridged particles and finally formation of aggregates.

While results from dustiness testing initially were intended for relative ranking of the substance emission potential, recent research investigates its potential use in control banding and time-resolved exposure modelling (Paik et al. 2008; Tielemans et al. 2008; Cherrie et al. 2009; Schneider et al. 2011; Van Duuren-Stuurman et al. 2012; Levin et al. 2014). Reliable use of standard dustiness indices for control banding and exposure modeling requires that the powders are not affected by their storage history and use conditions, or that the tests are conducted at the same conditions as

the storage and use. The limited documentation that is currently available suggests that a wider range in conditions during dustiness testing may be necessary. Previous studies did reveal important variation in dustiness with humidity for pharmaceutical powders, which are known to be hygroscopic and more susceptible to changes (Pujara 1997).

The primary aims of this study were

- (1) To investigate to what degree the dustiness levels and dust characteristics of slightly water-soluble and insoluble inorganic powders and different chemical surface modifications may be affected during storage at low, medium and high relative humidity without and with a physical pressure-load.
- (2) To assess the consequences of the results for risk assessment and management by comparison of assessment results using dustiness data from standard and non-standard incubation conditions.

All dustiness tests were conducted using the down-scaled EN15051 rotating dustiness drum which already has been used in a range of studies (Schneider and Jensen 2008; Jensen et al. 2009; Singh et al. 2011; Rasmussen et al. 2013, 2014; Levin et al. 2014) and currently is under evaluation as a standard method for dustiness testing of nanomaterial powders (Witschger et al. 2014).

The potential impact of the results on risk assessment was discussed using the obtained dustiness data in the NanoSafer control banding and risk management tool (<http://nanosafer.i-bar.dk/>, Kristensen et al. 2010) comparing the deviation from assessment results from standard and non-standard incubation conditions.

Methods and materials

Sample materials

Five different commercial inorganic nanostructured materials with slightly different primary particle sizes, morphologies, negligible to low water-solubilities, and some with and without chemical surface modifications were investigated within the study (Table 1).

The powders originate from the EU FP7 project HINAMOX in which the current study was planned to increase understanding on the potential variability in exposure potentials during different storage conditions for these specific powders.

All test materials were received as powders and stored in air-tight containers until the time of experiments. The nanomaterials were previously reported to vary in particle size-ranges and states of aggregation (Table 1) (data from Pérez-Campaña et al. 2012, 2013). The average primary particle size varied from a few nm to 36 nm, but the size distributions were generally wide and polydisperse. Only ZnO #1 had a nearly monodisperse size distribution. The primary particles were mainly aggregated in all samples. One of the samples, TiO₂, was surface-modified during production using HNO₃,

Although all of the sample materials are generally considered very low- to insoluble, literature data state solubility of ZnO between 4.88 and 7.40 mg/L (Xia et al. 2008; Reed et al. 2012; Li et al. 2012). Schmidt and Vogelsberger (2006) investigated solubility of TiO₂ and found that three commercially available nanosized TiO₂ had a solubility of 250 nmol/L (19.97 mg/L) at pH 1.5. The study also concluded that TiO₂ solubility increases with decreasing pH of medium and material primary particle size. This is of great importance as the TiO₂ sample in this study is stabilized by HNO₃, which is expected to render the surface to become highly hydroscopic. However, the effect may also include chemical destabilization and increased solubility. No literature values on solubility were found for CeO₂ and Al₂O₃.

The specific surface areas of the bulk nanopowders were measured using the BET (Brunauer–Emmett–Teller) nitrogen adsorption method. The materials were degassed for 72 h at 25 °C and subsequently analysed using Quantachrome Nova 4200 multipoint BET.

Surface analysis of the powders by X-ray photoelectron spectroscopy (XPS) was performed in a SPECS SAGE HR 100 system spectrometer on as-received powders. The X-ray source for TiO₂ was Mg K α (non-monochromatic, operated at 12.5 kV and 250 W). For other powders, experiments are performed with an Al K α source (non-monochromatic, operated at 12.5 kV and 300 W). The take-off angle was fixed at 90° and the measurements were conducted at a pressure of $\sim 10^{-6}$ Pa. Survey spectra

Table 1 Key physicochemical characteristics of the test nanomaterials

Sample	Source	Primary size (nm)	Characteristics	Specific surface area (m ² /g)	Surface composition (XPS)	Surface modification	Density (g/cm ³)	S ₀ (mg/L)
ZnO #1	Plasmachem GmbH	13.2 ± 5.4	Monodisperse, aggregated, spherical	26.2	16.9 % C, 50.9 % O, 32.2 % Zn	NA	5.61	4,88–7,40
ZnO #2	Degussa/Quimidroga	36.1 ± 18.1	Polydisperse, aggregated	21.9	20.7 % C, 43.8 % O, 35.5 % Zn	NA	5.61	4,88–7,40
Al ₂ O ₃	Plasmachem GmbH	13.6 ± 8.4	Polydisperse, aggregated	76.3	5.5 % C, 46.1 % O, 48.4 % Al	NA	3.95	NA
CeO ₂	Degussa/Quimidroga	13.0 ± 12.1	Polydisperse	56.7	22.1 % C, 60.8 % O, 17.0 % Ce	NA	7.2	NA
TiO ₂	Plasmachem	1–10	Aggregated	173.1	21.5 % C, 42.2 % O, 36.3 % Ti	HNO ₃ stabilized	4.23	NA

were obtained with a pass energy of 30 eV. Detailed spectra were acquired for C 1s, O 1s and metal regions (Ti 2p, Zn 2p, Ce 2s and Al 2p) with a pass energy of 15 eV. Spectra were analysed with the CasaXPS 2.3.15dev87 software. The analysis consisted of satellite removal, Shirley background subtraction, calibration of the binding energies to the C 1s C–C peak at 285 eV, and peak fitting with Gaussian–Lorentzian line shapes to determine the atomic percentages and chemical states of elements contained in each powder. The results from XPS characterisation are presented in Table 1.

Total carbon is assigned to adventitious carbon (Barr and Seal 1995), a carbonaceous material found on the surface of most samples exposed to air. Stoichiometric ratio (O/metal) is calculated from oxygen assigned to the metal oxide and the total metal contribution. Titanium analysis results with 85 % of Ti IV, while 15 % is assigned to Ti III or lower oxidation states, which explains the O/Ti ratio of 1.2. In the case of both zinc powders, the O/Zn ratio is 1 as expected, with a slightly higher amount of adventitious carbon for ZnO #2 powder. In the Ce 3d spectra, peaks are assigned to two oxidation states: Ce IV and Ce III (Engelhard et al. 2004). The ratio of Ce⁴⁺/Ce³⁺ is found to be 77/23, which corresponds to a higher O/Ce ratio, of 2.7. Aluminum quantification results in a O/Al ratio of 1 instead of the expected 1.5. This could be a result of inefficient oxidation of the aluminum precursor in the preparation process (Haerberle et al. 2013).

Experimental design of the incubation

The strategy for analysing the standard dustiness levels and the potential role of storage conditions was to test the powder dustiness at three different relative humidities (30, 50 and 70 % RH), each tested with and without a physical compaction of the powder. The case of 50 % RH without compaction constitutes as the standard test within the EN15051. A value of 70 and 30 % RH was selected as the upper and lower normal boundary conditions in workplaces handling. The uniaxial pressure load was selected to be 160 kg/m², which corresponds approximately to the load pressure experienced by the bottom layer bags on a single Euro-pallet with 15 bags (five layers).

The samples tested at “standard 50 % RH conditions” were stored in darkness at laboratory room

conditions with 50 % RH and equilibrated in the test system for 3 min before testing was commenced in the rotating drum. This procedure is prescribed in EN15051.

The experiments with fully controlled humidities with/without uniaxial pressure were completed by incubating the samples for 7 days in an incubator using a 2 lpm inlet flow with a controlled RH of 30, 50 or 70 %, respectively. The variation in RH was measured to be ± 2 %. The incubations were made by distributing the powder evenly in a flat-bottomed glass petri dish. Samples subjected to pressure load were weighed out in the same manner, and kept in the incubator for 24 h before the load was applied in order to ensure that the whole powder sample had equilibrated with the selected humidity conditions. The 2.7 kg load was applied on the inverted lid from the petri dish (14 cm OD) placed on top of the powder. The setup is illustrated in Fig. 1.

Dustiness testing

Data on dustiness for different materials and storage conditions were obtained using the down-scaled EN15051 dustiness drum as described in (Schneider and Jensen 2008). The humidifier and the sampling train were modified from the original design (Schneider and Jensen 2008) to allow simultaneous real-time measurement and sampling using up to five different samplers and to allow respirable dust fraction measurements by optionally inserting a GK2.69 cyclone (BGI, UK). For the humidity and pressure load experiments, an incubation chamber was connected in between the humidifier and the test chamber to ensure the same test conditions (Fig. 2).

In this study, real-time measurements were done for particle concentration and size distribution using the following systems:

- Fast Mobility Particle Sizer (FMPS 3091, TSI Inc., Shoreview, MN, USA) for particles in the range



Fig. 1 Illustration of powder placement in the incubation experiments where the *left*- and *right*-hand image shows the petri dish for pure humidity and combined humidity–pressure load incubations, respectively

5.6–560 nm. The measurement with the FMPS is done through combining size classification by electrical mobility and counting by particle charge after positive charge equilibration at a unipolar diffusion charger at the column inlet. To ensure no particle concentrations above the instrument limit, a recirculating HEPA-filtered 1:10 dilution system was placed in front of it.

- Aerodynamic Particle Sizer (APS 3321, TSI Inc., Shoreview, MN, USA), range 542 nm–20 μ m. The particle size measured with the APS is an aerodynamic equivalent sizes where the reference is a sphere with a density of 1. To ensure no particle concentrations above the instrument limit, it was coupled with a 1:20 dilution system (3302A, TSI Inc., Shoreview, MN, USA).
- Sampling on grids for transmission electron microscopy (TEM) was done in parallel for all materials and conditions using a mixed cellulose ester (MCE) 0.8- μ m filter-cassette for asbestos sampling with a holey-carbon-film-coated Cu-grid mounted on the MCE filter. Sampling was done from one of the outlet sampling lines using conductive tubing and performed at 1.5 lpm for 60 s. Due to insufficient loading of particles on TEM grids and later recognized uncertainties regarding their size-resolved sampling efficiencies, data from this work will only be presented in supplemental material.
- Respirable dust (PM₄) was sampled at 4.2 lpm on Teflon filters mounted in 0.8- μ m Millipore dust sampling cassettes after the GK2.69 cyclone.

The standard dustiness tests were conducted at 50 % RH according to EN 15051 with the adjustment that sampling was continued 120 s after termination of powder agitation. This has been normal practise in tests using the small rotating drum even though the original EN15051 standard procedure sampling is to be terminated immediately after the rotation has been stopped. The reason for the prolonged measurement time is that we have observed that the dust cloud decays long time after rotation are stopped. Hence, a full analysis of the generated dust requires prolonged sampling time to collect the whole dust cloud.

All experiments were conducted at 11 rpm and a horizontal flow rate of 11 lpm to obtain the same number of powder parcels falling per minute and average horizontal flow velocity in the cylinder as in

the EN 15051 test, respectively. HEPA-filtered and humidified air was supplied to the drum inlet and exhausted to be distributed into the different sampling units at the other end of the drum (Fig. 2).

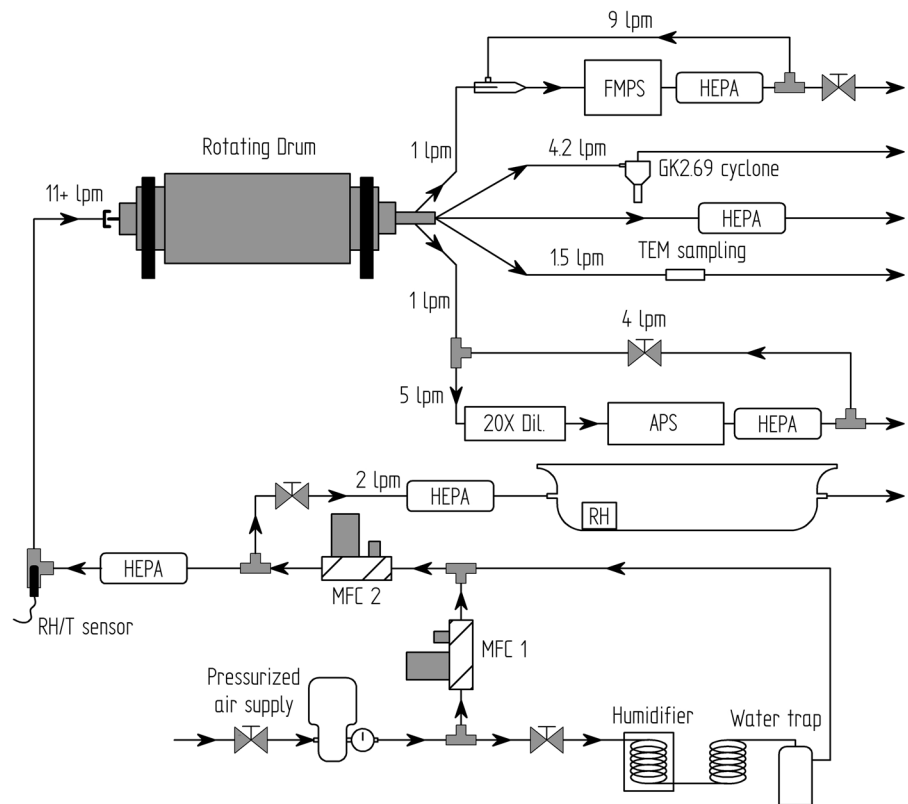
Loading of powders was done by first removing the exit cone of the drum and orient the drum with a lifter vane placed at lowest position of the rotation circle. As is the standard procedure in small rotating drum tests, 6 g of powder was carefully loaded in a pile on the upward moving side at the centre of the lifter vane. Then the system was closed, the humidity conditioned air-flow was applied and all flows were checked. The experiment was then initiated by leading the test atmosphere through the chamber for 180 s, during which the particle monitors reach background particle concentration levels and the dustiness test was initiated. After 60 s of rotation, the drum was stopped and sampling was maintained 120 s of particle sampling without rotation. This completed the rotation part of the dustiness test. Immediately after the conclusion of the test, the filter from the cyclone was retrieved. The mass of collected respirable dust was determined after

conditioning the exposed filters and filter controls in a weighing room (22 °C; 50 % RH) using a Sartorius microbalance (Type R162 P; Sartorius GmbH, Göttingen, Germany). The measured mass was corrected for handling and conditional variations through the use of blind filters. The limit of quantification, calculated as three times the standard deviation of the blind filters, was 0.20 mg. The weighed mass was then used to calculate and categorize the dustiness levels of the powders according to EN15051.

Data treatment of dustiness data

All real-time measurements were done using an assumed density of 1 g/cm³. FMPS and APS number concentrations were exported as $dN/d\log D_p$ values for each particle size, D_p . Measured data were corrected for background based on the 40 s average size spectra sampled before the test was initiated. All reported size distributions are the average accumulated size distributions over the whole duration of the experiment based on three repeats ($N = 3$). For determination of

Fig. 2 The experimental setup of the dustiness drum, incubation chamber and real-time monitors



respirable dustiness, the differential mass measured on the filters was corrected for variations in the three blank control filters and divided by the actual mass of the tested sample. The final value is an average of three repeats. The respirable dustiness index (mg/kg) is then calculated as the amount of dust (mg) collected on the filter divided by the amount (kg) of the test material and multiplied by a factor of 4.2/11 to match total flow through the drum.

Measurement of adsorbed water and water uptake

As water uptake can occur by adsorption as well as due to chemical reaction with the samples, the extent of this was investigated using different methods. The amount of water adsorbed at 50 % RH standard conditions was determined as described in the EN15051 standards specification. Due to limited sample availability, the water uptake at the three incubation conditions was done only at 30, 50 and 70 % RH without pressure load. After 7 days incubation, triplicates of ca. 0.5 g powder were weighed into glass petri dishes and placed in an oven for 4 h at 110 °C, removed and weighed out immediately. The mass loss during heat treatment was assumed to correspond to the amount of adsorbed water alone. An attempt was also made to determine the hygroscopicity and point of condensation of water on the test materials by environmental scanning electron microscopy using a Peltier cooling stage in a FEI ESEM Quanta 200 FEG (FEI, Eindhoven, the Netherlands). However, the results did not show any immediate

condensation until very high (>93.5 % RH) relative humidity (see supplemental material).

Consequences for risk assessment

To assess the potential consequences of the observed influences of storage conditions for risk assessment and associated risk management, a series of analyses were made for different principle exposure scenarios using the NanoSafer control banding and risk management tool. In this model, the exposure assessment is based on first-order exposure assessment modeling using dustiness data or default high values as one of the critical source strength input parameters. The tests were conducted using the dustiness values measured at 30, 50 and 70 % RH without loading to determine the NanoSafer exposure control band for each case. The tool has 5 exposure control bands ranking from 1 to 5 and is calculated for both process near-field and work room far-field concentrations for both Acute (15 min) and Chronic (8 h) exposure durations.

The studied scenarios were as follows:

- Small-scale activity; pouring of 5×2 kg into a mixer in a $3.5 \times 5 \times 2.9$ m³ workroom
- Intermediate scale activity; pouring of 5×20 kg into a mixer in a $4 \times 5 \times 3.5$ m³ workroom
- Large-scale industrial use activity; pouring one 800 kg big-bag into a dissolver in a $5 \times 10 \times 5$ m³ workroom.

More details of the scenario are collected in Table 2.

Table 2 Input parameters for three occupational exposure scenarios used in NanoSafer

	Scenario 1	Scenario 2	Scenario 3
Activity description-source domain	Scooping/filling bags in small-scale production	Pouring powder into twin-screw extruder	Wet mixing in dissolver
Activity energy factors level	0.1	0.5	0.75
Total amount used in the process	10 kg (5×2 kg)	100 kg (5×20 kg)	800 kg (1×800 kg)
Duration of the all process	75 min	30 min	5 min
Period between each cycle	6 min	1 min	0
Frequency of the process	1 time per day	1 time per day	1 time per day
Amount per each cycle	2 kg	20 kg	800 kg
Duration of each cycle	10 min	5 min	5 min
Room size	$3.5 \times 5 \times 2.9$	$4 \times 5 \times 3.5$	$5 \times 10 \times 5$
Ventilation rate	1 h^{-1}	5 h^{-1}	20 h^{-1}

It should be noted that control banding tools by definition do not give a quantitative values, but a qualitative precautionary risk assessments based on variable levels of quantitative and qualitative input and modelling depending on the tool. The aim of the test performed here is to illustrate through use of a real exposure assessment tool how important the observed differences caused by different storage conditions could be for exposure assessments.

Results and discussion

Gravimetric respirable dustiness index

Dustiness testing showed a large variation in the respirable dustiness levels of the powders tested under standard EN15051 conditions (3 min, 50 % RH, no load) and is shown in Fig. 3, denoted as '50 %'. The lowest levels of respirable dustiness were observed for

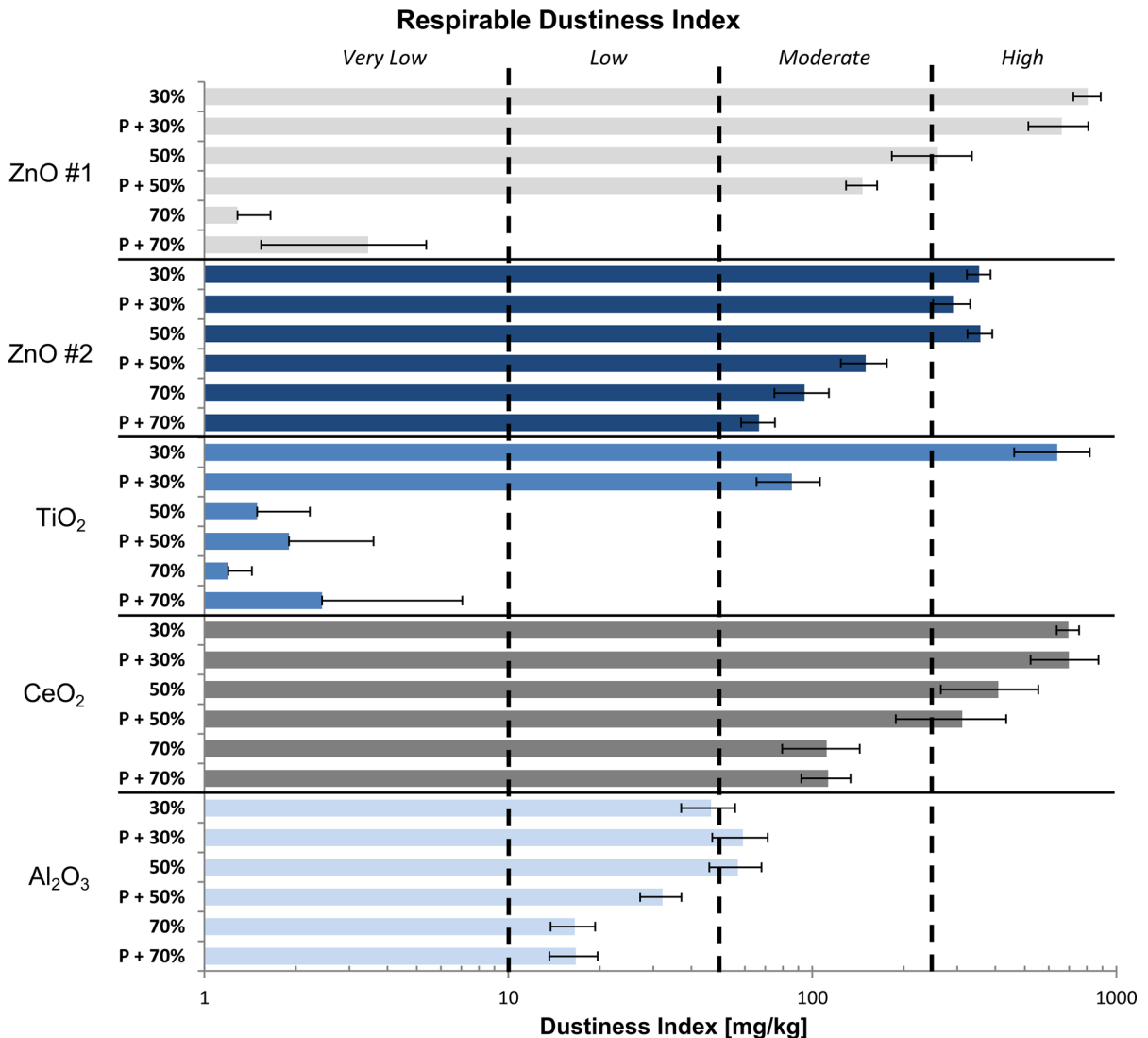


Fig. 3 Respirable dustiness index obtained at the different % RH and pressure load conditions. The percentage indicates relative humidity and 'P' the presence of 160 kg/m² pressure

during incubation. The dustiness ranks are based on the thresholds in the EN15051 standard

TiO₂ (<limit of quantification) and Al₂O₃ (56.9 mg/kg). The highest levels were observed for CeO₂ (409 mg/kg), ZnO #1 (259 mg/kg) and ZnO #2 (357 mg/kg). The EN15051 convention for classifications of powder dustiness denotes indices as *Very Low* for <10 mg/kg, *Low* for between 10 and 50 mg/kg, *Moderate* between 50 and 250 mg/kg and *High* >250 mg/kg as indicated in Fig. 3. Hence, the standard dustiness tests reveal that two powders are categorized as *Very Low* (TiO₂) and *Moderate* (Al₂O₃) and three (CeO₂, ZnO #1 and ZnO #2) are in the category of powders with *High* dustiness.

Testing the influence of storage conditions showed different effects on the respirable dustiness indices, depending on the sample material (Fig. 3). Dustiness of Al₂O₃ was reduced or unaltered reducing the humidity, whereas the index was lowered to less than 60 % by compaction at 50 % humidity. Increasing RH to 70 % caused a more severe drop in dustiness. ZnO #2 followed almost the same pattern, however, with greater reduction in dustiness due to compaction at both 30 (19 % reduction), 50 % RH (58 % reduction) and 70 % RH (29 % reduction). ZnO #1 showed a similar behaviour at 30 % RH and 50 % RH, but at 70 % RH, there is an extreme drop in dustiness index (<10 mg/kg) for both the compressed and uncompressed versions. CeO₂ was seemingly unaffected by physical loading at all levels of RH and moderately lowered in dustiness with increasing RH. The most dramatic effect was observed with TiO₂ which went from below limit of quantification at 50 and 70 % RH to 85.7 and 693.3 mg/kg for compacted and uncompactd at 30 % RH, respectively. TiO₂ is the HNO₃ stabilized material, and based on our

observations, incubation at these flow-through atmospheres caused release of corrosive vapours, which is ascribed to loss of the acidic HNO₃ stabilization.

All five materials had a statistically significant higher dustiness index at 30 % RH than at 70 % RH, both for compacted and uncompactd versions. A trend of higher values for 30 than 50 % RH can also be observed; however, it is not significant in all cases. No general pattern could be observed for changes in dustiness due to compaction, but in most cases compaction of the material decreased the dustiness. However, at higher humidities, the compaction appears to increase the dustiness. This might be due to compaction of the material limiting the uptake of water.

Water uptake

The measured water contents in the incubated powders are shown in Fig. 4 together with the corresponding dustiness indices. For ZnO #1 and TiO₂, there is a clear relation between increased water content and decreased dustiness index. Only small differences in water content for the different incubation humidities can be seen for the remaining three materials. For TiO₂, the high water uptake at all conditions, as compared to the other materials in the study, may be linked to the small primary particle size and high specific surface area.

Size distributions

All materials gave a typical bi-modal size-distribution at standard conditions with a smaller mode at

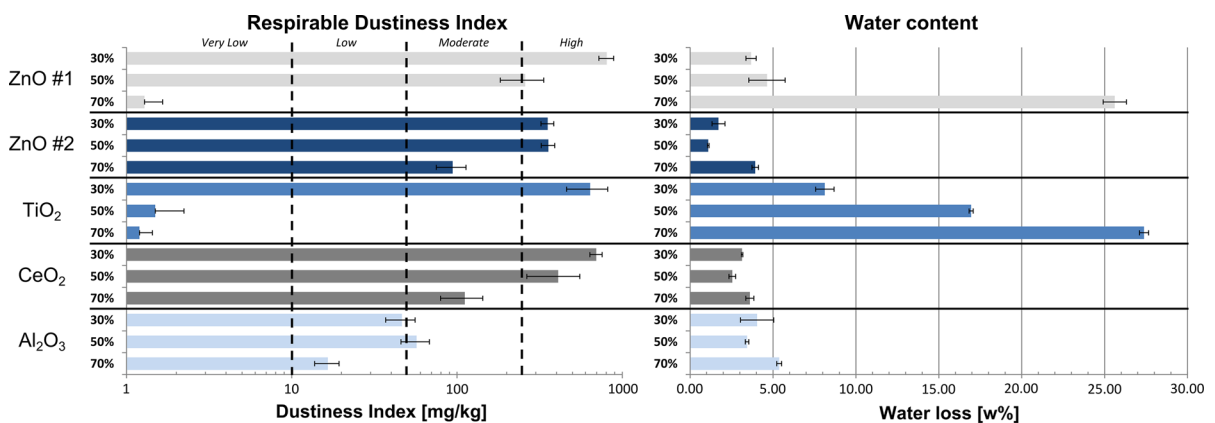


Fig. 4 Dustiness indices and water content of the five materials incubated at 30, 50 and 70 % RH

150–200 nm and a coarser at 2–3 μm , similar to size distributions reported in previous studies (Schneider and Jensen 2008; Jensen et al. 2009; Burdett et al. 2013; Levin et al. 2014). Figure 5 presents the accumulated size distributions as measured with FMPS and APS of TiO_2 and Al_2O_3 at 30, 50 and 70 % RH without loading to exemplify typical behaviour. Size distributions of all materials and storage conditions are available in supplemental material. The behaviour of the particle concentrations is well matched with that of the dustiness index, and the increase/decrease in particle numbers appears to be similar for all sizes. Presented data on particles <40 nm are due to electrometer noise accumulated over the course of the measurements.

Consequences for risk assessment

Table 3 presents the NanoSafer exposure risk-level bands obtained for the potential acute and chronic, near-field and far-field exposure levels for each powder and incubation conditions, respectively. It should be noted that NanoSafer consists of 5 bands for the allocation of the exposure potential ranking from 1 the lowest to 5 the highest. All materials give different

control bands in one or more of the three scenarios due to incubation humidity. In two of the cases ($\text{ZnO}\#1$ and TiO_2), a 20 % change in RH changes the exposure rank from the lowest to the highest level. For $\text{ZnO}\#1$, this occurs when changing the % RH from 50 to 70 in scenario 2 and 3. For TiO_2 , the drastic change in exposure rank is observed when going from 30 to 50 % RH in all three scenarios. The drastic effects can be observed in both near- and far-field concentrations and acute and chronic exposure times. The results from testing the powders in the NanoSafer control banding and risk management tool clearly show that the relative humidity and storage load play an important role on the emission potential of nanomaterial powders. In the worst case, an exposure- or risk-level estimated based on dustiness data produced under conditions different from reality may be extremely over- or underestimated depending on the material. This highlights the fact that the use of a single standard dustiness source term for control banding or quantitative exposure assessment may be critical if the test conditions vary considerably from the storage and use conditions. Unless such considerations are considered as safety margins or adopted into the tools or the dustiness data are actually generated

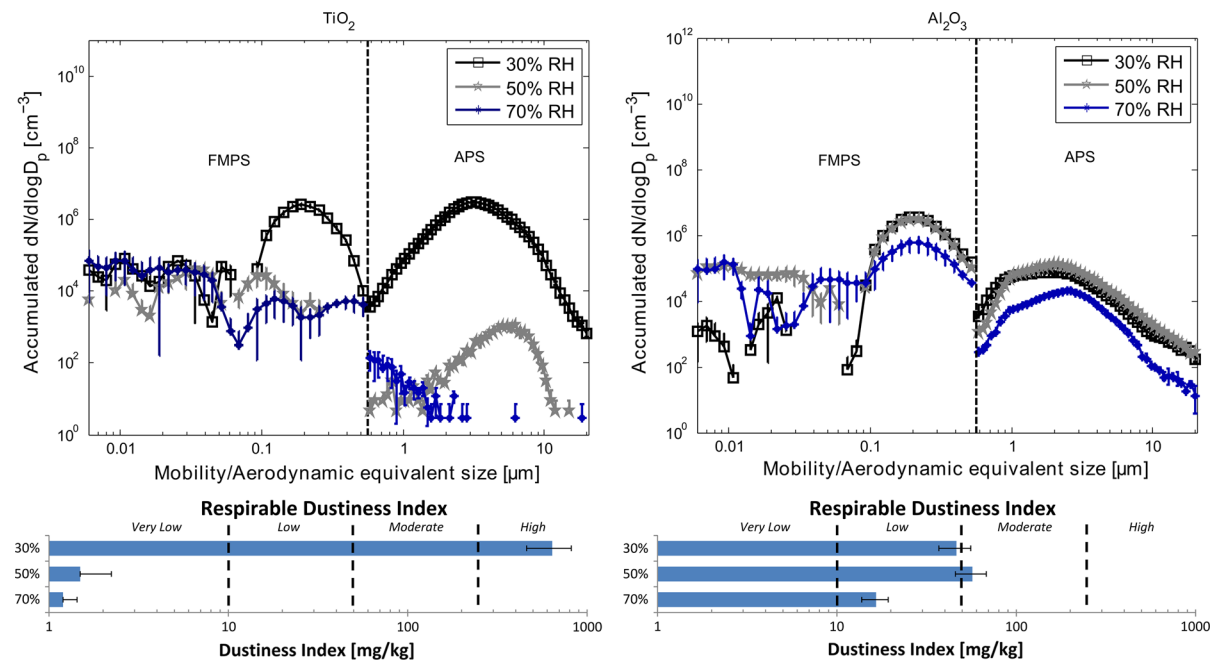


Fig. 5 Size distributions and corresponding gravimetrical dustiness levels of TiO_2 and Al_2O_3 at 30, 50 and 70 % RH

Table 3 NanoSafer exposure risk-level bands for acute exposure (15 min) and chronic exposure (8 h) calculated for each test material and incubation conditions

%RH	Scenario 1				Scenario 2				Scenario 3				
	Near Field		Far Field		Near Field		Far Field		Near Field		Far Field		
	Acute	Chr.	Acute	Chr.	Acute	Chr.	Acute	Chr.	Acute	Chr.	Acute	Chr.	
ZnO ₁	30	4	3	3	3	5	5	5	5	5	5	5	5
	50	2	2	2	1	5	5	5	5	5	5	5	5
	70	1	1	1	1	1	1	1	1	3	1	1	1
ZnO ₂	30	3	3	3	2	5	5	5	5	5	5	5	5
	50	3	3	3	2	5	5	5	5	5	5	5	5
	70	1	1	1	1	5	5	5	4	5	5	5	5
Al ₂ O ₃	30	1	1	1	1	4	2	4	2	5	4	5	2
	50	1	1	1	1	5	2	4	2	5	5	5	3
	70	1	1	1	1	3	1	2	1	5	3	5	1
TiO ₂	30	5	5	5	4	5	5	5	5	5	5	5	5
	50	1	1	1	1	2	1	1	1	5	2	3	1
	70	1	1	1	1	2	1	1	1	5	2	3	1
CeO ₂	30	4	4	4	4	5	5	5	5	5	5	5	5
	50	4	3	4	3	5	5	5	5	5	5	5	5
	70	2	2	2	1	5	5	5	5	5	5	5	5

under comparable conditions, these effects add a major uncertainty to the results of exposure assessment.

Conclusions and recommendations

In this study, the effects of storage conditions such as relative humidity and physical loading on the dustiness of five inorganic nanomaterials were investigated. Gravimetric dustiness index and particle size distributions were measured using rotating drum tests. Long-term water uptake of the powders was found to be an explanatory factor of the changes. Consequences of these varying storage conditions in exposure modelling were tested using the control banding and risk management tool NanoSafer.

The study shows that there is a material-dependent change in the dustiness index due to both humidity conditions and physical load during 7 days simulated storage. A general trend of reduced dustiness index with increased relative humidity was observed, although the magnitude varies with the materials. The effect of physical loading is more complicated, but the magnitude of the change is also generally smaller than that of the humidity condition.

The most severe effect was seen on the TiO₂ material which had a dustiness index below detection limit at standard dustiness conditions but ranked in as

Very high (693.3 mg/kg) at 30 % RH incubation. This suggests that the effect of storage humidity on dustiness can be severe for certain powders and that the ±10 % RH gap allowed for in the EN15051 might be too broad. In this case, the major effect is ascribed to the HNO₃ stabilization used for this product.

Testing the consequences of the observed variation in dustiness using the NanoSafer control banding/risk management tool using three work scenarios also showed great variability in the exposure assessment. Of greatest concern, assessments based on high humidity conditions would seriously underestimate the need for increased ventilation and personal protection equipment compared to the same scenario at low humidity conditions.

To reduce the uncertainties associated with the effects of humidity during storage and work, we suggest that dustiness testing for exposure assessment should be expanded to include tests that also target the extreme ranges of the relative humidity at workplaces. Moreover, the allowed variation around the specified humidity levels should be reduced considerably from 10 % as given today in EN15051 and data on storage conditions may be essential. If data are to be used for more accurate predictive modelling, dustiness data on additional test conditions may be needed. Further studies to determine the effect of % RH in more detail are required to define more precisely the critical boundaries for the test conditions.

Acknowledgments This work was conducted as part of the Strategic Research effort at the National Research Centre for the Working Environment and the Danish Centre for Nanosafety (20110092173/3) from the Danish Working Environment Research Foundation and the EU Framework seven Programme HINAMOX (228825).

References

- Aitken RA, Bassan A, Friedrichs S et al (2011) Specific advice on exposure assessment and hazard/risk characterisation for nanomaterials under REACH (RIP-oN 3)
- Barr TL, Seal S (1995) Nature of the use of adventitious carbon as a binding energy standard. *J Vac Sci Technol A* 13:1239–1246. doi:[10.1116/1.579868](https://doi.org/10.1116/1.579868)
- Borm PJ, Robbins D, Haubold S et al (2006) The potential risks of nanomaterials: a review carried out for ECETOC. *Part Fibre Toxicol* 3:11. doi:[10.1186/1743-8977-3-11](https://doi.org/10.1186/1743-8977-3-11)
- Brockel U, Wahl M, Kirsch R, Feise HJ (2006) Formation and growth of crystal bridges in bulk solids. *Chem Eng Technol* 29:691–695
- Brouwer D (2010) Exposure to manufactured nanoparticles in different workplaces. *Toxicology* 269(2):120–127
- Brouwer DH (2012) Control banding approaches for nanomaterials. *Ann Occup Hyg* 56:506–514. doi:[10.1093/annhyg/mes039](https://doi.org/10.1093/annhyg/mes039)
- BS EN:15051 (2006) EN15051 Workplace atmospheres: measurement of the dustiness of bulk materials—requirements and reference test methods
- Burdett G, Bard D, Kelly A, Thorpe A (2013) The effect of surface coatings on the dustiness of a calcium carbonate nanopowder. *J Nanoparticle Res* 15:1311. doi:[10.1007/s11051-012-1311-9](https://doi.org/10.1007/s11051-012-1311-9)
- Cherrie JW, Gillies AT, Sleuwenhoek A et al (2009) Modelling exposure to pharmaceutical agents. *J Phys Conf Ser* 151(1):012063
- Engelhard M, Azad S, Peden CHF, Thevuthasan S (2004) X-ray photoelectron spectroscopy studies of oxidized and reduced CeO₂(111) surfaces. *Surf Sci Spectra* 11:73–81. doi:[10.1116/11.20050201](https://doi.org/10.1116/11.20050201)
- Freitag F, Kleinebudde P (2003) How do roll compaction/dry granulation affect the tableting behaviour of inorganic materials? Comparison of four magnesium carbonates. *Eur J Pharm Sci* 19:281–289
- Gbureck U, Dembski S, Thull R, Barralet JE (2005) Factors influencing calcium phosphate cement shelf-life. *Biomaterials* 26:3691–3697
- Haeberle J, Henkel K, Gargouri H et al (2013) Ellipsometry and XPS comparative studies of thermal and plasma enhanced atomic layer deposited Al₂O₃-films. *Beilstein J Nanotechnol* 4:732–742. doi:[10.3762/bjnano.4.83](https://doi.org/10.3762/bjnano.4.83)
- Hamelmann F, Schmidt E (2005) Methods for dustiness of industrial powders. *China Particuol* 03:90–93
- Hämeri K, Lähde T, Hussein T et al (2009) Facing the key workplace challenge: assessing and preventing exposure to nanoparticles at source. *Inhal Toxicol* 21(Suppl 1):17–24. doi:[10.3109/08958370903202804](https://doi.org/10.3109/08958370903202804)
- Jensen KA, Koponen IK, Clausen PA, Schneider T (2009) Dustiness behaviour of loose and compacted Bentonite and organoclay powders: what is the difference in exposure risk? *J Nanoparticle Res* 11:133–146
- Kristensen HV, Jensen KA, Koponen IK et al (2010) Nanopartikler i arbejdsmiljøet - Viden og inspiration om håndtering af nanomaterialer. Industriens Branchearbejdsmiljøråd, Branchearbejdsmiljørådet for Undervisning og Forskning samt Universitets og Bygningsstyrelsen, Copenhagen
- Kuhlbusch TAJ, Asbach C, Fissan H et al (2011) Nanoparticle exposure at nanotechnology workplaces: a review. *Part Fibre Toxicol* 8:22. doi:[10.1186/1743-8977-8-22](https://doi.org/10.1186/1743-8977-8-22)
- Levin M, Koponen IK, Jensen KA (2014) Exposure assessment of four pharmaceutical powders based on dustiness and evaluation of damaged HEPA filters. *J Occup Environ Hyg* 11:165–177. doi:[10.1080/15459624.2013.848038](https://doi.org/10.1080/15459624.2013.848038)
- Li X, Lenhart JJ, Walker HW (2012) Aggregation kinetics and dissolution of coated silver nanoparticles. *Langmuir* 28:1095–1104. doi:[10.1021/la202328n](https://doi.org/10.1021/la202328n)
- Liden G (2006) Dustiness testing of materials handled at workplaces. *Ann Occup Hyg* 50:437–439
- Liguori B, Hansen SF, Baun A, Jensen KA (Submitted) Comparative analysis of occupational exposure estimation tools for nanomaterials and their applicability for reach
- Nishii K, Horio M (2007) Chapter 6 Dry granulation. In: Salman AD (ed) *Handbook of Powder Technology*. Elsevier Science B.V., pp 289–322
- Paik SY, Zalk DM, Swuste P (2008) Application of a pilot control banding tool for risk level assessment and control of nanoparticle exposures. *Ann Occup Hyg* 52:419–428
- Pérez-Campaña C, Gómez-Vallejo V, Martin A et al (2012) Tracing nanoparticles in vivo: a new general synthesis of positron emitting metal oxide nanoparticles by proton beam activation. *Analyst* 137:4902–4906. doi:[10.1039/C2AN35863H](https://doi.org/10.1039/C2AN35863H)
- Pérez-Campaña C, Gómez-Vallejo V, Puigivila M et al (2013) Biodistribution of different sized nanoparticles assessed by positron emission tomography: a general strategy for direct activation of metal oxide particles. *ACS Nano* 7:3498–3505. doi:[10.1021/nm400450p](https://doi.org/10.1021/nm400450p)
- Pujara CP (1997) Determination of factors that affect the generation of airborne particles from bulk pharmaceutical powders. Theses Diss Available ProQuest pp 1–155
- Rasmussen K, Mech A, Mast J et al (2013) Synthetic amorphous silicon dioxide (NM-200, NM-201, NM-202, NM-203, NM-204): characterisation and physico-chemical properties JRC Repository: NM-series of representative manufactured nanomaterials
- Rasmussen K, Mast J, de Temmerman P-J et al (2014) Titanium dioxide, NM-100, NM-101, NM-102, NM-103, NM-104, NM-105: characterisation and physico-chemical properties
- Reed RB, Ladner DA, Higgins CP et al (2012) Solubility of nano-zinc oxide in environmentally and biologically important matrices. *Environ Toxicol Chem* 31:93–99. doi:[10.1002/etc.708](https://doi.org/10.1002/etc.708)
- Schmidt J, Vogelsberger W (2006) Dissolution kinetics of titanium dioxide nanoparticles: the observation of an unusual kinetic size effect. *J Phys Chem B* 110:3955–3963. doi:[10.1021/jp0553611](https://doi.org/10.1021/jp0553611)
- Schneider T, Jensen KA (2008) Combined single-drop and rotating drum dustiness test of fine to nanosize powders using a small drum. *Ann Occup Hyg* 52(1):23–34

- Schneider T, Brouwer DH, Koponen IK et al (2011) Conceptual model for assessment of inhalation exposure to manufactured nanoparticles. *J Expo Sci Environ Epidemiol* 21:450–463
- Singh C, Friedrichs S, Levin M et al (2011) NM-series of representative manufactured nanomaterials—zinc oxide NM-110, NM-111, NM-112, NM-113: characterisation and test item preparation
- Szepvolgyi J, Mohai I, Gubicza J (2001) Atmospheric ageing of nanosized silicon nitride powders. *J Mater Chem* 11: 859–863
- Tardos GI (2005) Wet-granulation research with application to scale-up. *China Particuol* 3:191–195
- Tielemans E, Schneider T, Goede H et al (2008) Conceptual model for assessment of inhalation exposure: defining modifying factors. *Ann Occup Hyg* 52:577–586
- Van Duuren-Stuurman B, Vink SR, Verbist KJM et al (2012) Stoffenmanager nano version 1.0: a web-based tool for risk prioritization of airborne manufactured nano objects. *Ann Occup Hyg* 56(5):525–541
- Witschger O, Jensen KA, Brouwer DH et al (2014) DUSTI-NANO: a CEN pre-normative research project to harmonize methods for manufactured nanomaterial powders. *Aerosol Technology* 2014, Karlsruhe. Abstract T230A09. Session APPVI Dustiness and Resuspension: <http://www.gaef.de/AT2014/>
- Xia T, Kovoichich M, Liang M et al (2008) Comparison of the mechanism of toxicity of zinc oxide and cerium oxide nanoparticles based on dissolution and oxidative stress properties. *ACS Nano* 2:2121–2134. doi:10.1021/mn800511k